W-band Finite Ground Coplanar Waveguide (FG-CPW) using Laser Enhanced Direct-Print Additive Manufacturing (LE-DPAM)

Mohamed M. Abdin[1#], W. Joel D. Johnson[2], Jing Wang[1], Thomas M. Weller[3]
[1]Department of Electrical Engineering, University of South Florida, Tampa, FL, USA
[2]Harris Corporation, Dept. of Antenna-RF Systems Engineering, Palm Bay, FL, USA
[3]School of Electrical Engineering and Computer Science, Oregon State University, Corvallis, OR, USA
[#]mabdin@mail.usf.edu

***Abstract* — Design, fabrication, and measurement of finite ground coplanar waveguides (FG-CPWs) operating up to 110 GHz is demonstrated using additive manufacturing (AM) technology. FG-CPWs were fabricated using laser enhanced direct-print additive manufacturing, where laser-machining at 355 nm or 1064 nm wavelength was employed along with fused deposition modeling and micro-dispensing in a single digital manufacturing platform. This approach provides high dimensional accuracy that is required by mm-wave packaging systems. The characterization of laser machining at wavelengths of both 355 nm and 1064 nm was examined with specific focus on the feature size and dimensional accuracy. Several FG-CPW designs for 50 and 60 ohms are characterized and compared against a FG-CPW line on a commercially available calibration substrate. Attenuation as low as ~0.3 dB/mm at 110 GHz is achieved. To the best of the authors' knowledge, this is the first reported experimental result for transmission lines at W-band using laser enhanced direct-print additive manufacturing (LE-DPAM).**

***Keywords*—millimeter wave, 3D Printing, FG-CPW, W-band, additive manufacturing, laser machining, 110 GHz, transmission lines.**

I. Introduction

The push for fifth generation (5G) and millimeter wave (mm-wave) applications requires cost-effective yet high performance fabrication and packaging techniques [1]. Additive manufacturing (AM) technologies such as aerosol jet printing (AJP), inkjet printing, and micro dispensing [2]-[10] are viable for the fabrication of multilayer packages and interconnects with low manufacturing cost. With continued improvements, the size and performance of additive manufactured interconnects are now comparable to those of multilayer printed circuit boards (PCB). Specifically, laser enhanced direct-print additive manufacturing (LE-DPAM) is demonstrated as a viable technology for manufacturing interconnects that operate up to 110 GHz.

As with other AM approaches, LE-DPAM combines low production costs with fast turn-around time. The pico-second laser used in LE-DPAM achieves high accuracy for features as small as 5 μm while improving the performance of the transmission lines. The approaches help to overcome some of the main challenges for AM fabrication such as low conductivity metals, low resolution in the printing features, and maintaining tight tolerances for the circuit dimensions.

In this paper, the design, fabrication, and characterization of a digital manufactured finite ground coplanar waveguide (FG-CPW) is presented that operates from 0-110 GHz. With a single LE-DPAM platform, fused deposition modeling of ABS and micro-dispensing of silver paste (DuPont CB028) were combined with pico-second pulsed laser machining at a wavelength of 355 nm or 1064 nm for digital manufacturing of the proposed mm-wave FG-CPWs. Transmission line losses as low as ~0.3 dB/mm at 110 GHz, which is on par with that of a FG-CPW counterpart on an alumina calibration substrate, is demonstrated.

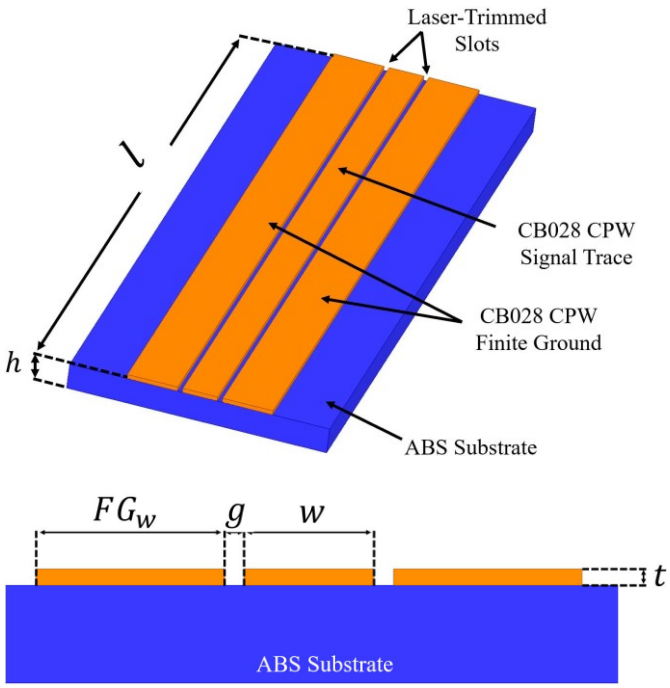

Fig. 1. Isometric and cross-sectional view of the proposed AM FG-CPW.

II. Design and Fabrication

A. Design guidelines for FG-CPW

The FG-CPW scheme was selected over other conventional coplanar waveguide structures due to its reduced size and lower susceptibility to the excitation of higher modes at mm-wave frequencies. Several lines based on the configuration shown in Fig. 1 were designed with different characteristic impedances. Design restrictions for the key dimensions of the CPW line (e.g., width *w* and gap *g*) were followed to achieve optimal

performance. To avoid resonances due to the finite width of the substrate and any packaged walls that the transmission lines may be enclosed in, the ground plane width, FG_w, should be less than $\lambda_g/4$ at the highest operating frequency, where λ_g is the guided-wavelength ($\lambda_o/\sqrt{\varepsilon_r}$) [11]. When FG_w is larger than twice the center conductor width, w, both the line attenuation (a) and the effective permittivity of the CPW become largely independent of the width of the grounds. To mitigate radiation losses and keep dispersion small, the upper limit of the ground width is designed to be less than $\lambda_g/8$. The sum of the two gap widths, g, and the center conductor width, *w*, is considered the total line width of the CPW line and should be smaller than $\lambda_g/4$ to suppress coupling to parasitic modes. The substrate thickness, *h*, is selected to be 0.5 mm such that it is much larger than the gap width, while also providing structural support.

These design constraints result in dimensions much smaller than what can be achieved by the micro-dispensing of the silver paste. However, pico-second pulsed laser post-deposition trimming can be used to achieve features as small as 5 µm consistently. The conductor thickness, t, can be controlled by the height of the micro-dispenser nozzle over the substrate and can be varied between 25 µm to 80 µm to be used as an additional design parameter to control the characteristic impedance. The additively manufactured CPW dimensions are summarized in Table 1 and compared to other CPW lines.

B. Fabrication Process

The fabrication process was carried out with an nScrypt 3Dn tabletop system capable of a 0.5 µm alignment resolution. This is a standalone digital manufacturing platform that combines fused deposition modelling, micro-dispensing, and laser machining. Acrylonitrile butadiene styrene (ABS), a thermoplastic with $\varepsilon_r = 2.35$ and $\tan = 0.0065$ measured at 30 GHz [5], is used for the dielectric substrate, where the ABS filament is extruded through a 240°C heated 200 µm inner-diameter nozzle on a 110°C heatedbed. The conductor traces are printed using Dupont CB028 conductive silver paste that is micro-dispensed using a 75 µm inner-diameter nozzle onto the printed ABS substrate and dried in-situ on the heating bed at

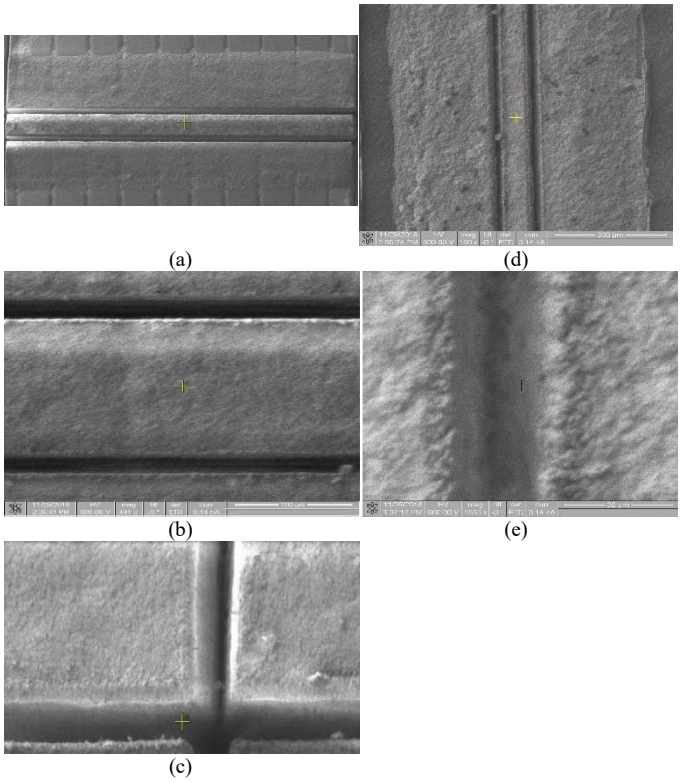

Fig. 2. SEM images of AM FG-CPW machined with (a)-(c) 355 nm and (d)-(e) 1064 nm wavelength laser. (c) The slot width is 15 µm with ~25 µm-thick silver paste that has smooth wall surfaces.

100°C for 1 hour achieving a 2 MS/m conductivity [5]. The slots of the FG-CPW are cut using a Nd:YAG (Lumera Laser's SUPER RAPID-HE) pico-second pulsed laser beam at a repetition rate of 100 kHz using either the 355 nm wavelength using an average power (P_{avg}) from 0.025 W to 0.65 W or the 1064 nm wavelength using a P_{avg} of 2.4 W. When using the 1064 nm wavelength, the beam can be focused down to ~12-15 µm spot diameter but the cut results in relatively rough wall surfaces and a limited aspect ratio of around 2:1 as shown in Fig. 2 (e).

Table 1. Summary of CPW Lines' Features, Dimensions, and Measurement Results Compared with other Transmission Lines

Work	Z_o **(Ω)**	w **(µm)**	g **(µm)**	FG_w **(µm)**	t **(µm)**	L **(mm)**	**Frequency (GHz)**	**Attenuation (dB/mm)**	**Process and Structure**
*This work**	60	80	20	260	25	12	110	0.355	LE-DPAM CPW using 1064nm
	50	160	20	260	25	2	110	0.6	LE-DPAM CPW using 355nm
	60	135	30	260	25	2	110	0.298	LE-DPAM CPW using 355nm
*CS-5***	50	50	25	230	~2	6.6	110	0.46	Gold on alumina PCB lithography CPW
[5]	50	300	20	1500	25	1.5	40	0.35	LE-DPAM CPW using 1064nm
[6]	50	29.5	16.3	~30	1.5	0.8	40	0.7	AJP on alumina CPW
[7]	50	51	32	600	1.4-4	2	110	0.45	AJP CPW-microstrip-CPW
[8]	50	51	NA	NA	2-3	2-6.6	110	0.5	Rapid micro-product development (RMPD) microstrip
[9]	50	~35	40	~120	NA	~0.45	110	0.4	Inkjet on LCP CPW

**h= 0.5 mm for all AM designs.*
***CS-5 is a commercially available calibration substrate*

In comparison, the 355 nm wavelength beam can be focused down to a spot size of 5 µm, producing smoother walls with a higher aspect ratio as shown in Fig. 2 (c). As a result, better control of feature size and improved repeatability are possible. The dimensional accuracy and fabrication tolerance within a few microns are important for implementation of FG-CPW operating at mm-wave frequencies. Moreover, the laser machining process also sinters the trimmed sidewall edges within the CPW gaps, thus improving the effective conductivity of the silver paste [5]. When compared to the K-band AM CPW fabricated on a Rogers' substrate [5], the CPW reported in this paper is fabricated using only AM technology and maintains good operation up to 110 GHz. The high frequency performance is capable due to the accurate slot widths with higher aspect ratio by using the 355 nm wavelength instead of 1064 nm, and due to following the design guidelines to avoid exciting higher-modes at higher frequencies.

III. Simulation and Measurements

A. Measurement Setup

The FG-CPW lines were characterized using an Agilent PNA-N5227A network analyser and GGB 150 µm-pitch picoprobes from 0-67 GHz. Subsequently, measurements from 65-110 GHz were performed using 3742A-EW Anritsu W-band extenders. The broadband frequency response was combined with a 2 GHz overlap to ensure data consistency. The multi-line through-reflect-line (mTRL) probe tip calibration using a GGB CS-5 calibration substrate was performed. A glass slide with a thickness of 1 mm was placed beneath the devices under test and the calibration substrate to avoid microstrip modes at higher frequencies due to the metal chuck of the probe station.

B. Results

Fig. 3 shows the measured attenuation per unit length and return loss of the FG-CPW from DC up to 110 GHz for 50- and 60-ohm characteristic impedances using a laser machining wavelength of 355 nm or 1064 nm. The results are plotted against those for a FG-CPW 50-Ω line from the CS-5 alumina calibration substrate. The plot shows a close agreement between measured and simulated frequency responses for all AM CPW lines.

The 3D EM simulations were performed using Ansys HFSS 19. For accurate simulation results, the walls of the laser-machined slots were given a different conductivity than the conductivity of non-sintered regions of CB028 away from the cutting regions indicated as S_t in Fig. 4. For the CPW lines cut with the 355 nm laser, S_t is 1.5 µm-wide adjacent to the slots and is assigned a conductivity of approximately 10^7 S/m. For the lines cut with the 1064 nm laser, 2 µm-wide regions with bulk silver conductivity of 6.1 x 10^7 S/m were found to compare best to measured results. Additionally, the dielectric loss was modeled using Djordjevic-Sarkar model for wide-band operation. The removal of some ABS during the laser-cutting of the CPW slots creates an air-filled cavity underneath the slots that is approximately 10-15 µm deep and represented as C_d in

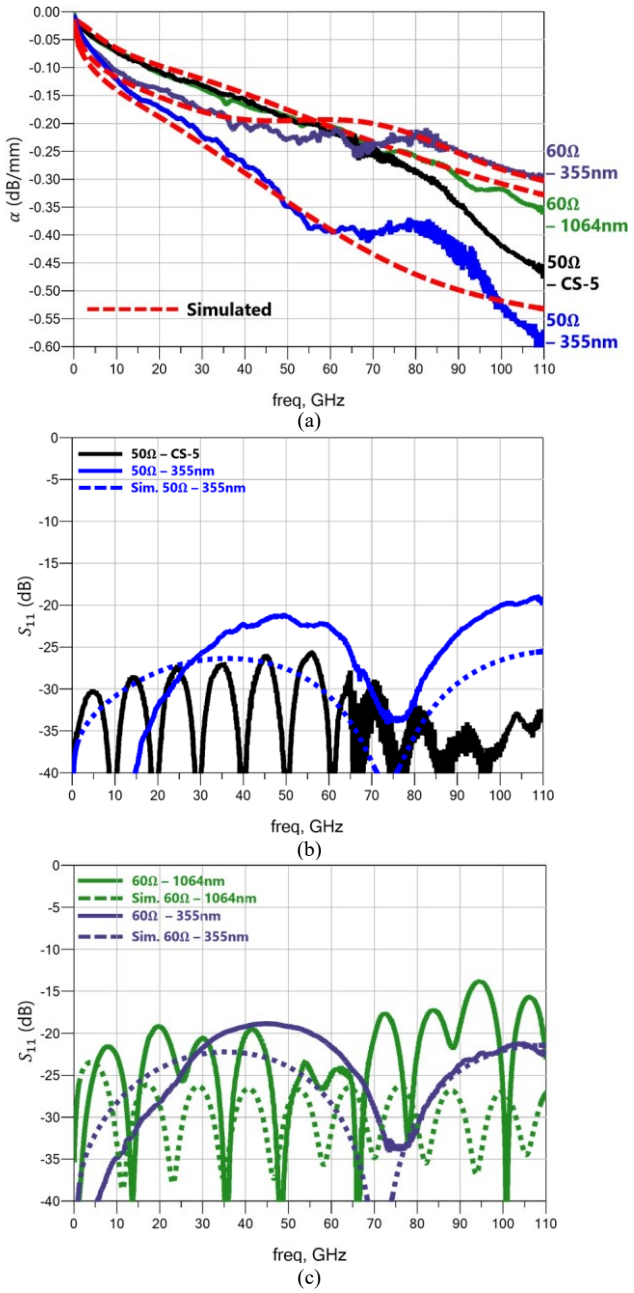

Fig. 3. Measured and simulated (a) attenuation and (b-c) return loss for (b) 50 Ω and (b) 60 ∧ AM CPW lines compared with 50 Ω CPW on CS-5 alumina calibration substrate. AM CPW lines are laser machined using 355 nm and 1064 nm wavelengths.

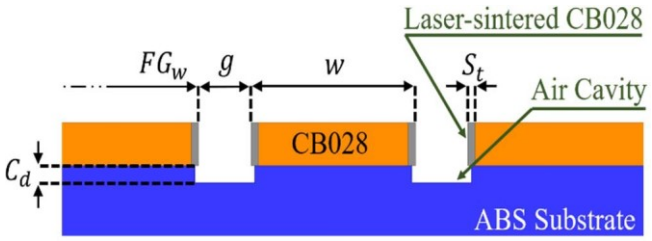

Fig. 4. 3D EM model representing CPW post-laser trimming. Air cavities and higher-conductivity regions were added to represent real structure.

Fig. 4. Since the slots are narrow to enable high frequency operation, the fields are mostly concentrated along the gap and air cavities and there is a resulting decrease in the effective permittivity of the lines. These additions in the simulation setup result in excellent agreement with measurement performance for the different characteristic impedances.

By observing the attenuation and return losses of the additively manufactured FG-CPW plotted against the FG-CPW from the CS-5 calibration substrate, several conclusions can be reached:

1. The AM FG-CPW lines show comparable performance to a FG-CPW device on the commercial calibration substrate built by traditional fabrication techniques with 0.3 dB/mm attenuation at 110 GHz.
2. Return loss under 15 dB indicates excellent repeatability and accuracy of the LE-DPAM fabrication process for slots as small as 15 µm.
3. Excellent fit to the data across a wide bandwidth shows accurate EM modelling and well characterized materials.
4. Based on experimental results and simulations comparing different characteristic impedances using Keysight's ADS 2016 method of moments impedance analyzer, 60-Ω seems to be preferred over other characteristic impedances when using ABS and CB028.

IV. Conclusion

The performance of several additively manufactured FG-CPW lines with varied characteristic impedance is demonstrated with measured attenuation that is on par with traditional manufactured counterparts on an alumina calibration substrate at frequencies from DC to 110 GHz. The results are further validated using 3D EM simulations with good agreement. Two wavelengths of a pico-second laser, 355 and 1064 nm, were investigated for post-processing of lines that are printed using fused deposition modelling and micro-dispensing. FG-CPW lines with 50-60 Ω characteristic impedances demonstrate good mm-wave performance and fabrication repeatability. Excellent wideband performance with losses as low as 0.3 dB/mm were measured at 110 GHz. Simulations indicate that the same transmission lines can operate up to ~170 GHz before higher order modes are excited.

Acknowledgments

The authors are grateful for the assistance from Modelithics, Inc with the W-band measurement setup.

References

[1] M. M. Abdin, W. Joel D. Johnson and T. M. Weller, "A system and technology perspective on future 5G mm-wave communication systems," 2017 IEEE 18th Wireless and Microwave Technology Conference (WAMICON), Cocoa Beach, FL, 2017, pp. 1-6.

[2] F. Cai, Y.-H. Chang, K. Wang, C. Zhang, B. Wang, and J. Papapolymerou, "Low-loss 3-D multilayer transmission lines and interconnects fabricated by additive manufacturing technologies," IEEETrans. Microw. Theory Techn., vol. 64, no. 10, pp. 3208–3216, Oct. 2016. [2]

[3] C. Mariotti, F. Alimenti, L. Roselli, and M. M. Tentzeris, "High performance RF devices and components on flexible cellulose substrate by vertically integrated additive manufacturing technologies," IEEE Trans. Microw. Theory Techn., vol. 65, no. 1, pp. 62–71, Jan. 2017

[4] T. P. Ketterl, Y. Vega, N. C. Arnal, J. W. I. Stratton, E. A. Rojas-Nastrucci, M. F. Córdoba-Erazo, M. M. Abdin, C. W. Perkowski, P. I. Deffenbaugh, K. H. Church, and T. M. Weller, "A 2.45 GHz Phased Array Antenna Unit Cell Fabricated Using 3-D Multi-Layer Direct Digital Manufacturing," in IEEE Transactions on Microwave Theory and Techniques, vol. 63, no. 12, pp. 4382-4394, Dec. 2015

[5] E. A. Rojas-Nastrucci, H. Tsang, P. I. Deffenbaugh, R. A. Ramirez, D. Hawatmeh, A. Ross, K. Church, and T. M. Weller, "Characterization and Modeling of K-Band Coplanar Waveguides Digitally Manufactured Using Pulsed Picosecond Laser Machining of Thick-Film Conductive Paste," in IEEE Transactions on Microwave Theory and Techniques, vol. 65, no. 9, pp. 3180-3187, Sept. 2017

[6] A. Delage, N. Delhote, S. Verdeyme, B. Bonnet , L. Carpentier, C. Schick, T. Chartier, C. Chaput, "Aerosol jet printing of millimeter wave transmission lines on 3D ceramic substrates made by additive manufacturing," 2018 IEEE/MTT-S International Microwave Symposium - IMS, Philadelphia, PA, 2018, pp. 1557-1560.

[7] M. T. Craton, J. Sorocki, I. Piekarz, S. Gruszczynski, K. Wincza and J. Papapolymerou, "Realization of Fully 3D Printed W-Band Bandpass Filters Using Aerosol Jet Printing Technology," 2018 48th European Microwave Conference (EuMC), Madrid, Spain, 2018, pp. 1013-1016

[8] T. Merkle, R. Götzen, J. Choi and S. Koch, "Polymer Multichip Module Process Using 3-D Printing Technologies for D-Band Applications," in IEEE Transactions on Microwave Theory and Techniques, vol. 63, no. 2, pp. 481-493, Feb. 2015.

[9] J. Kimionis, S. Shahramian, Y. Baeyens, A. Singh and M. M. Tentzeris, "Pushing Inkjet Printing to W-Band: An all-printed 90-GHz beamforming array," 2018 IEEE/MTT-S International Microwave Symposium - IMS, Philadelphia, PA, 2018, pp. 63-66.

[10] S. Yang, S. Zhen and A. Shamim, "Fully Inkjet Printed 85GHz Band Pass Filter on Flexible Substrate," 2018 48th European Microwave Conference (EuMC), Madrid, 2018, pp. 652-654.

[11] E. Ponchak, George & Tentzeris, Manos & Katehi, Linda. (1997). Characterization of Finite Ground Coplanar Waveguide with Narrow Ground Planes. International Journal of Microcircuits and Electronic Packaging. 20. 167-172.